

Computing solid angle using perimeter points

Russell P. Patera¹

351 Meredith Way, Titusville, FL 32780, United States

Abstract

The solid angle of a region can be computed as the rotational transformation of an axis after its tip slews about the solid angle region once while its base remains fixed at the observer location. The transformation can be achieved by moving the tip of the axis from perimeter point to point sequentially using great circle arcs until it returns to its original orientation. This method works very well for spherical polygon shapes, but has reduced accuracy when the perimeter is curved. Increasing the number of points that define the perimeter improves accuracy but can also introduce numerical roundoff error. The proposed method uses both slewing and rotational motion of the axis to define the contour of the solid angle region more accurately. This new method results in greater accuracy while using fewer perimeter points. Numerical examples are included to illustrate the method.

Keywords: solid angle, Ishlinskii's theorem, Attitude kinematics

Nomenclature

| | |
|------------------|---|
| A | semi-major axis of ellipse |
| B | semi-minor axis of ellipse |
| h | distance from observer to the plane of the ellipse |
| p | x component shift of the observer |
| P_i | perimeter point vector |
| q | y component shift of the observer |
| Q_i | normal to perimeter point vector |
| R | radius of circular disk |
| U_i | incremental transformation linking perimeter points |
| U_R | rotational transformation |
| U_S | slewing transformation |
| U_T | total transformation |
| W_i | transformation to the i^{th} perimeter point |
| $\Delta\omega_i$ | incremental rotation along axis |
| ω_i | Euler Rotation Vector of U_i |
| $\Delta\omega_T$ | sum of incremental rotations |

1. Introduction

The attitude transformation method of solid angle calculation was developed in earlier works, Patera (2020a), Patera (2020b). The method is based on an axis whose tip slews about the solid angle region while its base remains fixed at the observation point. After the axis slews one complete revolution about the solid angle region. it will have acquired a rotation about its axis equal to the solid angle. This is in agreement with Ishlinskii's Theorem (1952), which states, if an axis fixed in the body, describes a closed conical surface in space, the angle of rotation of the body around this axis is equal to the integral of the projection of the angular velocity of the body onto this axis plus the solid angle of the cone enclosed. Since the axis slews about the region using a series of great circle arcs, there is no associated angular velocity along the axis itself. As a result, the residual rotation about the axis at the end of its transit is solely due to the enclosed solid angle. The method was shown to give accurate results for various published cases involving elliptical disk solid angle regions by using polygons to approximate the elliptical

¹ Russell.p.patera@gmail.com

disk region, Patera (2020b). However, since slewing the axis using great circle arcs, which is appropriate for polygons, does not precisely represent a curved shape, some error is introduced. Therefore, increasing the number of perimeter points is required to produce the desired accuracy. The Perimeter Point Method (PPM), presented in this work uses both slewing and rotational motion of the axis to define the trajectory of the axis between perimeter points more precisely. The resulting solid angle calculation has greater accuracy while using fewer perimeter points than the polygonal approximation method. Using only 3 perimeter points, the solid angle of a circular disk from any point along its normal axis was computed using PPM with only numerical roundoff error. It was successfully tested against published results from Conway (2010) and Thabet, et. al. (2020).

2. Computing solid angle using perimeter points

The perimeter of a solid angle region when viewed from a fixed observer can be defined by a consecutive set of vectors, \mathbf{P}_i , extending from the observer to the i^{th} perimeter point. Three consecutive vectors are used to define the transformation between the first two consecutive vectors. Using \mathbf{P}_1 and \mathbf{P}_2 , normal vectors, \mathbf{Q}_1 and \mathbf{Q}_2 , are obtained, as shown in eqs. (1) and (2).

$$\mathbf{Q}_1 = \mathbf{P}_1 \times \mathbf{P}_2 \quad (1)$$

$$\mathbf{Q}_2 = \mathbf{P}_1 \times \mathbf{Q}_1 \quad (2)$$

After normalizing \mathbf{P}_1 , \mathbf{Q}_1 and \mathbf{Q}_2 , the 3 x 3 transformation matrix \mathbf{W}_1 can be defined as shown in eq. (3).

$$\mathbf{W}_1 = (\mathbf{P}_1 \quad \mathbf{Q}_1 \quad \mathbf{Q}_2) \quad (3)$$

The process is repeated with the second and third perimeter vectors to obtain \mathbf{W}_2 , as shown in eqs. (4-6).

$$\mathbf{Q}_3 = \mathbf{P}_2 \times \mathbf{P}_3 \quad (4)$$

$$\mathbf{Q}_4 = \mathbf{P}_2 \times \mathbf{Q}_3 \quad (5)$$

$$\mathbf{W}_2 = (\mathbf{P}_2 \quad \mathbf{Q}_3 \quad \mathbf{Q}_4) \quad (6)$$

The transformation linking \mathbf{W}_1 and \mathbf{W}_2 is \mathbf{U}_1 and is obtained using eq. (7).

$$\mathbf{U}_1 = \mathbf{W}_2 \mathbf{W}_1^{-1} \quad (7)$$

This process is repeated using all the perimeter vectors in sequence until the final transformation increment is reached, which terminates with the original perimeter vector. The total transformation is computed, as shown in eq. (8) and is equal to a rotation of 360 degrees or 2π radians about the axis at its original orientation, which is also its final orientation.

$$\mathbf{U}_T = \mathbf{U}_1 \mathbf{U}_2 \mathbf{U}_3 \mathbf{U}_4 \dots \mathbf{U}_N = \mathbf{U}(\mathbf{P}_1, 2\pi) \quad (8)$$

The rotational transformation about the axis associated with each incremental transformation must be evaluated and summed to find the associated total rotational transformation. This can be achieved using a dot product of the incremental Euler Rotation Vector with the axis at each associated orientation. The Euler rotation vector, $\boldsymbol{\omega}_i$, is found from each \mathbf{U}_i using standard methods and used in eq. (9) to obtain the incremental axis rotation, $\Delta\omega_i$. Since it was shown in an earlier work, Patera (2020a), that the slewing and rotational transformations commute, the sum of the incremental rotations can be moved to the last axis orientation, \mathbf{P}_1 , as is shown in eq. (10). Therefore, the associated rotational transformation is given by eq. (11). Note that \mathbf{P}_1 is both the initial and final axis orientation.

$$\Delta\omega_i = \boldsymbol{\omega}_i \cdot \mathbf{P}_i \quad (9)$$

$$\Delta\omega_T = \sum_1^N \Delta\omega_i \quad (10)$$

$$\mathbf{U}_R = \mathbf{U}(\mathbf{P}_1, \Delta\omega_T) \quad (11)$$

The total transformation in eq. (8) is the product of the slewing transformation and the rotational transformation, as shown in eq. (12). Using eq. (8) and eq. (11) in eq. (12), the slewing transformation is given by eq. (13), where the inverse of the rotational transformation is obtained by the negative of the angle. The rotations in eq. (13) can be combined, since they are about the same axis, \mathbf{P}_1 .

$$\mathbf{U}_T = \mathbf{U}_S \mathbf{U}_R \quad (12)$$

$$\mathbf{U}_S = \mathbf{U}_T \mathbf{U}_R^{-1} = \mathbf{U}(\mathbf{P}_1, 2\pi) \mathbf{U}(\mathbf{P}_1, -\Delta\omega_T) = \mathbf{U}(\mathbf{P}_1, 2\pi - \Delta\omega_T) \quad (13)$$

The solid angle is the magnitude of the Euler Rotation Vector of \mathbf{U}_S and is also the residual rotation of the slewing axis after it completes one purely slewing circuit about the solid angle region. Therefore, the solid angle is identified as the rotation angle about \mathbf{P}_1 , as given in eq. (14).

$$\Omega = 2\pi - \Delta\omega_T \quad (14)$$

Eq. (14) is applicable to all types of solid angle shapes, including great circle arcs and conical shaped curves. The sharper the curve, the more perimeter points are needed to define the shape precisely.

3. Visualizing the perimeter contour

A triangle is used to illustrate how PPM generates a curve trajectory between perimeter points. Let an observer be located 20 meters along an axis normal to the plane of the triangle whose vertices are on the perimeter of a circular disc having a radius of 10 meters. Let the normal axis be coincident with the z-axis, which passes through the center of the circular disk. The perimeter points as viewed from the observer appear to be located in the x-y plane, as shown in Fig. 1, where each perimeter point is located at one of the vertices of the triangle.

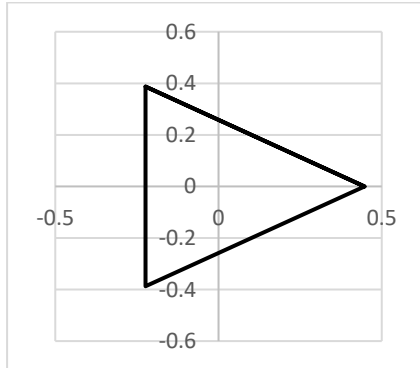


Fig. 1. Spherical triangle having 3 perimeter points as view from an observer normal to the axis.

If the perimeter points are connected by great circle arc slews, the solid angle is the magnitude of the Euler Rotation Vector of the slewing transformation of the axis after one complete circuit about the triangle. However, the trajectory of the axis follows a conical curve between perimeter points when PPM is used to compute the solid angle, as shown in Fig 2. Thus, PPM assumes a conical perimeter for the solid angle region when only 3 perimeter points are used. By adding additional points to define the triangle rather than the circular disk, PPM alters the perimeter contour to more nearly represent the triangular shape. Table 1 contains the extra number of points between each of the three perimeter points and the associated solid angle computed by PPM.

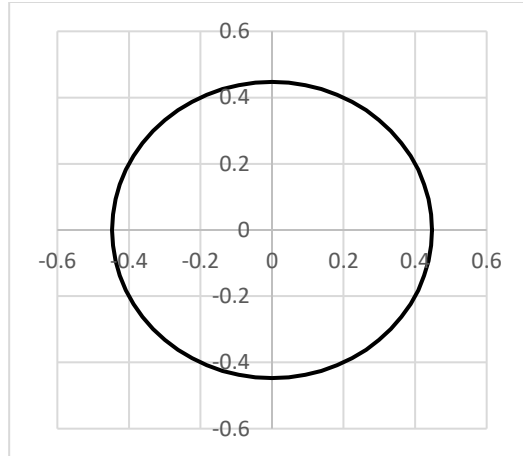


Fig. 2 Contour of spherical triangle shape having 3 perimeter points when using PPM.

Table 1. Extra points versus solid angle

| Number of Extra Points | PPM Solid Angle | Actual Solid Angle | Percent Difference |
|------------------------|-----------------|--------------------|--------------------|
| 1 | 0.6633 | 0.2976 | 122.876 |
| 2 | 0.3888 | 0.2976 | 30.638 |
| 3 | 0.3361 | 0.2976 | 12.930 |
| 4 | 0.3186 | 0.2976 | 7.050 |
| 6 | 0.3066 | 0.2976 | 3.017 |
| 8 | 0.3026 | 0.2976 | 1.673 |
| 16 | 0.2988 | 0.2976 | 0.397 |
| 32 | 0.2979 | 0.2976 | 0.094 |
| 360 | 0.297629 | 0.297627 | 0.003 |

Figs. (3-5) illustrate the contour shapes for representative cases found in Table 1. The more perimeter points that are used, the closer the contour approaches that of the spherical triangle rather than the circular disk.

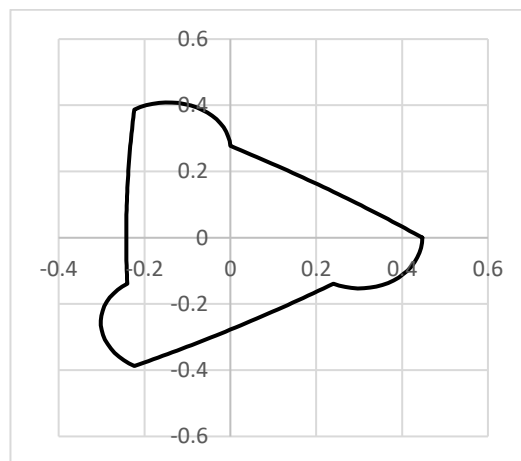


Fig. 3. PPM contour for 3 extra points between the 3 perimeter points.

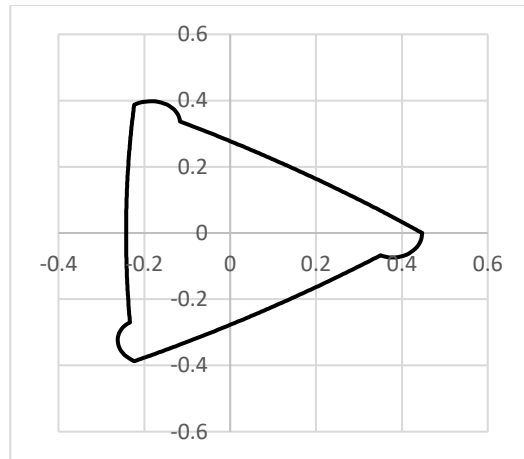


Fig. 4 PPM contour for 6 extra points between the 3 perimeter points.

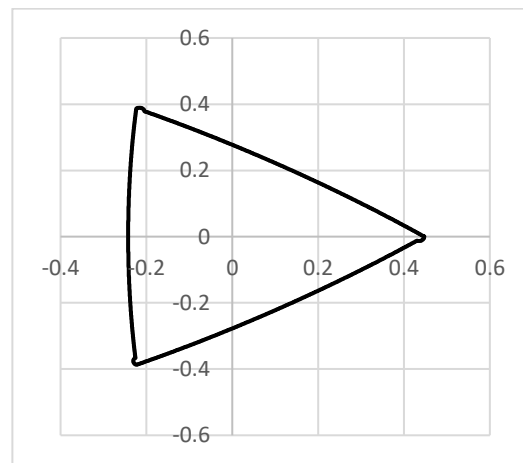


Fig. 5 PPM contour for 32 extra points between the 3 perimeter points.

The PPM solid angles in Table 1 represent the solid angles of the associated contours exactly except for numerical roundoff error. As the number of points increase, the PPM contour more closely represents the actual spherical triangle and the calculated solid angle approaches the actual solid angle, as shown in Table 1.

4. Numerical results

The new method to compute solid angle was implemented in several computer simulations to demonstrate its performance. Results of PPM were first compared to the exact solution of a simple known case involving an observer located on the axis of a circular disk. For an observer located at a distance h along the axis of a disk having radius R , the solid angle is given by eq. (15).

$$\Omega = 2\pi \left[1 - \frac{h}{\sqrt{R^2 + h^2}} \right] \quad (15)$$

Figure 6 shows the solid angle obtained using eq. (15), when $R = 10$ and h ranges from 0 to 200. The solid angle was also computed using the proposed method with a 3 symmetrically placed points on the perimeter of the circular disk. Figure 7 shows the percent difference between the solid angle found using PPM and the solid angle of the disk using the exact formula in eq. (15). Also shown for comparison purposes, are the results presented in an earlier publication that used a polygon shape of the same area to represent the disk, Patera (2020b). The solid angle of PPM is exact except for numerical processing errors. The polygon approximation method is very accurate

but not exact. In this case, PPM is exact because it assumes the perimeter points are on a conical curve, which they are in this simple case. The advantage of PPM is that the observer can be located at any point and does not have to be on the axis of the disk, as required by eq. (15). When the observer is off the axis of the disk, more perimeter points may be required to obtain sufficiently accurate results.

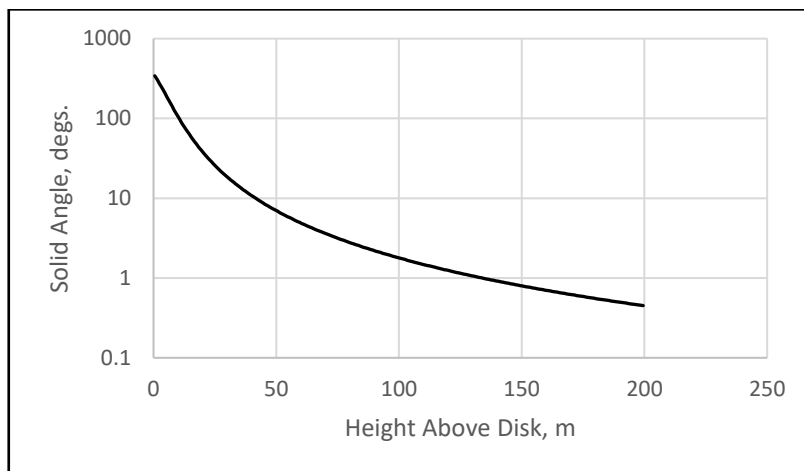


Fig. 6. Exact solid angle of a disk having radius of 10 meters with respect to a point above a disk along its axis.

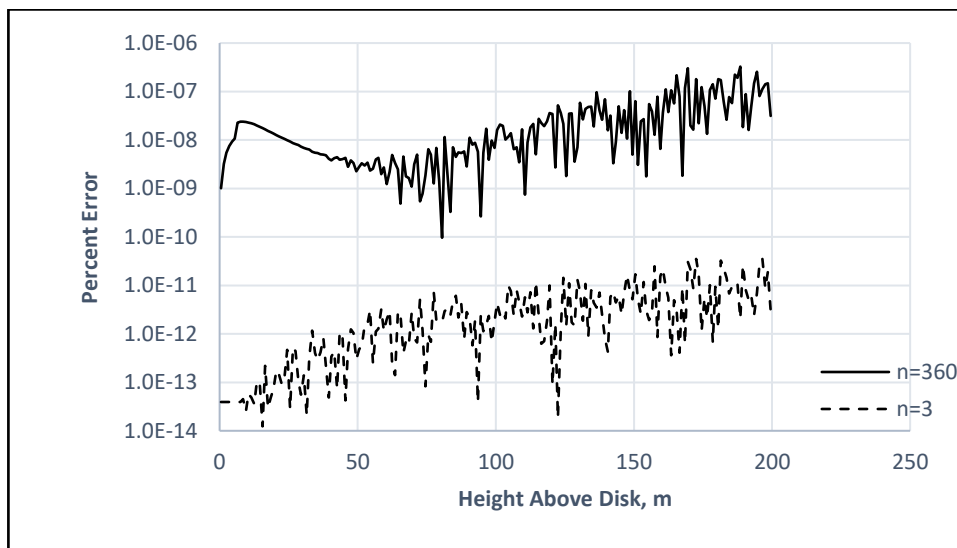


Fig. 7. Percent error of PPM when using 3 symmetrically positioned perimeter points on the circular disk and a polygonal approximate method that uses 360 perimeter points.

4.1 Observer on an axis of an elliptical disk

The proposed method can also be used to compute the solid angle of an elliptical disk with respect to a point source along the axis normal to the plane of the disk. Let A and B be the semi-major axis and semi-minor axes of the ellipse, respectively. In this case, perimeter points were space evenly on a circle of radius B and then the circle

and the associated perimeter points were stretched along the semi-major axis to define the desired ellipse. The resulting perimeter points were used in the processing presented in Section 2 to obtain the solid angle.

The results using PPM were compared to published results, Thabet, et. al. (2020) in Table 2, which includes results from Conway (2010). The results of PPM, when rounded down to seven digits to the right of the decimal point, agreed with the results of Conway (2010). All cases used 360 perimeter points. The number of points for case #4 was increased to 2600, as shown in parentheses, to match Conway's result exactly. The number of points for case #5 was increased to 1000 to match Conway's result exactly. Although cases #4 and #5 are numerically stressful cases, PPM can achieve higher accuracy by increasing the number of perimeter points defining the solid angle region. The only limitation is numerical processing error.

Table 2. Solid angle comparison for an ellipse with an observer located on its axis

| Case # | A | B | h | Conway (2010) | Thabet, et. al. (2020) | PPM (n=360) |
|--------|------|-------|------|---------------|------------------------|----------------------------------|
| 1 | 2 | 1 | 0.01 | 6.2347447 | 6.2346390 | 6.2347447 |
| 2 | 2 | 1 | 0.5 | 4.0425592 | 4.0423850 | 4.0425592 |
| 3 | 2 | 1 | 10 | 0.0616819 | 0.0616804 | 0.0616819 |
| 4 | 1000 | 1 | 1 | 3.1415778 | 3.1414940 | 3.1415626 [3.1415778, (n =2600)] |
| 5 | 100 | 1 | 1 | 3.1405637 | 3.1404830 | 3.1405676 [3.1405637, (n =1000)] |
| 6 | 1 | 0.99 | 1 | 1.8291325 | 1.8290270 | 1.8291325 |
| 7 | 1 | 0.2 | 1 | 0.4724316 | 0.4724257 | 0.4724316 |
| 8 | 1 | 0.01 | 1 | 0.0239619 | 0.0239632 | 0.0239619 |
| 9 | 1 | 0.001 | 1 | 0.0023963 | 0.0023972 | 0.0023963 |

4.2 Observer on an axis offset from the elliptical disk axis

The PPM can also handle cases where the observer is not located on the axis through the center of the ellipse, but is located on an axis parallel and offset by (p, q) from the central axis. Table 3 shows that PPM, while using 360 perimeter points, produces results in exact agreement to those of Conway (2010) for nearly all the cases. Three of the cases required more perimeter points to match Conway exactly. The results in Table 3 show that PPM is valid for observers located anywhere with respect to the ellipse.

Table 3. Solid angle for an ellipse with respect to an observer located at (p, q, h)

| Case # | A | B | p | q | h | Conway (2010) | PPM (n=360) |
|--------|-----|-----|-----|-----|------|---------------|----------------------------------|
| 1 | 1.5 | 1.0 | 0.6 | 0.5 | 0.1 | 5.4932906 | 5.4932906 |
| 2 | 1.5 | 1.0 | 0.6 | 0.5 | 2.52 | 0.5690505 | 0.5690505 |
| 3 | 1.5 | 1.0 | 0.6 | 0.5 | 10.0 | 0.0461472 | 0.0461472 |
| 4 | 1.0 | 4.0 | 2.0 | 0.5 | 0.1 | 0.1104206 | 0.1104206 |
| 5 | 1.0 | 4.0 | 0.1 | 4.0 | 5.0 | 0.2589691 | 0.2589691 |
| 6 | 2.0 | 1.0 | 1.0 | 0.5 | 1.0 | 1.9450789 | 1.9450788 [1.9450789 (n = 400)] |
| 7 | 2.0 | 1.0 | 5.0 | 1.0 | 1.0 | 0.0547517 | 0.0547517 |
| 8 | 3.0 | 1.0 | 1.0 | 0.5 | 0.5 | 3.6792113 | 3.6792110 [3.6792113 (n = 1800)] |
| 9 | 5.0 | 1.0 | 1.0 | 0.5 | 0.5 | 3.9166119 | 3.9166118 [3.9166119] (n = 600)] |
| 10 | 1.1 | 1 | 1 | 0.9 | 2.0 | 0.4744215 | 0.4744215 |

5. Conclusion

A method was developed to compute the solid angle by using perimeter points that bound the solid angle region. The method uses the fact that the solid angle is equivalent to the magnitude of the Euler Rotation Vector of the slewing transformation of an axis having one end fixed at the observer and the other end slewing once about the solid angle region. An earlier method used a polygonal approximation of the perimeter to obtain the purely slewing transformation and associate Euler Rotation Vector magnitude. Since the great circle arcs used in the polygonal approximation method do not represent curved contours precisely, some error is introduced. The perimeter point method developed in this work uses both the slewing and rotational transformation of the slewing axis to more accurately define the axis trajectory between perimeter points. This new method results in greater accuracy than the polygonal approximation method while using fewer perimeter points. Only 3 perimeter points were needed to compute the solid angle of a circular disk from any point along its normal axis. This was achieved with only numerical roundoff error, since the slewing axis defines a conical shape, which is implicit in the perimeter point method. Computer programs were developed to compare numerical results to published results involving circular and elliptical disk shapes. Results showed that the perimeter point method has accuracy equal to, or better than published methods while often using fewer points. The perimeter point method is applicable to solid angle regions of any shape, and is not restricted to elliptical or polygonal solid angle regions.

References

Conway, J. T., "Analytical solution for the solid angle subtended at any point by an ellipse via a point source radiation vector potential," *Nuclear Instruments and Methods in Physics Research A* 614, 17-27 (2010).

Ishlinkskii, A. Yu., "The Mechanics of Special Gyroscopic Systems," *Izd. Akad. Nauk, UkrSSR, Kiev*, (1952).

Patera, R. P., "Attitude kinematics using slewing transformation of a single axis," *Advances in Space Research*, 66 1460-1474, (2020a).

Patera, R., P., "General method of solid angle calculation using attitude kinematics," *ViXra:2008.0076*, <http://dx.doi.org/10.13140/RG.2.2.24471.60327> (2020b).

Thabet, A. A., Hamawy, A., and Badawi, M. S., "New Mathematical Approach to Calculate the Geometrical Efficiency Using Different Radioactive Sources with Gamma-ray Cylindrical Shape Detectors," *Nuclear Engineering and Technology* 52, Issue 6, 1271-1276, (2020).